

Layout influence on microwave performance of graphene field effect transistors

M.A. Giambra[✉], A. Benfante, L. Zeiss, R. Pernice, V. Miseikis, W.H.P. Pernice, M.H. Jang, J.-H. Ahn, A.C. Cino, S. Stivala, E. Calandra, A.C. Busacca and R. Danneau

The authors report on an in-depth statistical and parametrical investigation on the microwave performance of graphene FETs on sapphire substrate. The devices differ for the gate-drain/source distance and for the gate length, having kept instead the gate width constant. Microwave S -parameters have been measured for the different devices. Their results demonstrate that the cut-off frequency does not monotonically increase with the scaling of the device geometry and that it exists an optimal region in the gate-drain/source and gate-length space which maximises the microwave performance.

Introduction: Different configurations of graphene transistors have already been proposed in the literature, such as conventional planar metal-oxide-graphene field effect transistors (MOSFETs) structures, bilayer graphene, graphene nanoribbons MOS structures, and vertical transistors exploiting tunnelling mechanisms [1–3]. The effects of scaling down the gate-source, gate-drain distances and the gate length have already been studied for GaN-based high electron mobility transistors (HEMTs), SiC metal-semiconductor field effect transistors (MESFETs) [4, 5] as well as the role of the gate length for graphene-based transistors [6]. Graphene FET (GFET) performance improvement due to gate length reduction is not so obvious due to the possibility of adversely affecting transistor behaviour through parasitic doping by the metal/graphene contacts [7]. In the vicinity of the metal contacts, the invasive effects are stronger, leading to an asymmetry of the transfer characteristics, especially in short channels [8]. Obviously, such effect is expected to be lower for longer channels; however, a compromise has to be found in terms of device geometries. In particular, due to the capacitive effects in the high-frequency domain, both gate-drain/source distance and gate-length have to be considered. Up-to-date, literature reports parametrical studies concerning only the dependence of f_T on L_g without taking into account the effect on Δ . On the other hand, these geometrical factors, affecting GFETs parasitic elements, do play a fundamental role in the determination of the RF characteristics.

In this Letter, we present a statistical and parametrical investigation aimed at experimentally evaluating the microwave parameters dependence on GFET dimensions. Starting from the results already reported on the cut-off frequency scaling behaviour versus the channel length [9], our analysis has been carried out varying both the gate-drain/source distance and the gate length to study the layout influence on the devices' performance.

Results and discussion: Twenty-four GFET families, differing from each other only for the gate-drain/source distance (Δ) and the gate length (L_g), were fabricated on a single sapphire chip [10–12] (Fig. 1a). Each family includes ten nominally identical devices. GFETs dimensions (Δ and L_g) were chosen in the range [125 ÷ 175] and [125 ÷ 2000] nm, respectively, while the drain length and the channel width were kept constant at 3 and 20 μm , respectively. Moreover, in order to perform the de-embedding procedure, auxiliary test structures (open, short and thru-line) were fabricated on the same chip. After fabrication, GFETs were characterised in both the DC and RF/microwave regimes. DC measurements allowed us to obtain the static transconductance curves (I_D versus V_{GS}) and, hence, to evaluate the incremental low-frequency transconductance ($g_m = \partial I_D / \partial V_{GS} |_{V_{DS}=\text{const}}$), whose value deeply influences the whole device performance. DC curves for a device with $\Delta = 125$ nm, $L_g = 250$ nm, drain length = 3 μm , and channel width = 20 μm are shown in Fig. 1. In particular, Figs. 1b and c show I_D and g_m versus V_{GS} curves (parameterised in V_{DS}). Typical values for contact resistance, doping and field effect mobility were found to be ≈ 1.7 $\text{k}\Omega \cdot \mu\text{m}$, $\approx 5.4 \times 10^{12}$ cm^{-2} and ≈ 1600 cm^2/Vs , respectively. The values, extrapolated from measurements, are comparable to the typical ones reported for wet-transferred polycrystalline chemical vapour deposition (CVD) graphene devices with top contacts [13]. Significant improvements could be achieved by using single crystal graphene [14], alternative transfer methods [15] and edge contact [16].

Considering the variation of channel doping in each device, we identified the region with maximum g_m values, in which subsequent RF/microwave measurements were performed. The scattering parameters were then measured in the frequency range [50 MHz ÷ 20.05 GHz] in standard environmental conditions, using a HP8510C Vector Network Analyser and a Cascade Summit 9000 wafer-probe station. The de-embedding of the devices was performed through a combined use of electromagnetic simulations and experimental measurements on auxiliary test structures implemented on the same chip (open, short etc.). Typical short-circuit current gain ($|h_{21}|$) and maximum available gain (MAG) of an intrinsic device with $\Delta = 125$ nm and $L_g = 250$ nm, as calculated from the measured S -parameters (bias point: $V_{GS} = -0.2$ V; $V_{DS} = -2$ V), are depicted in Figs. 2a and b, respectively.

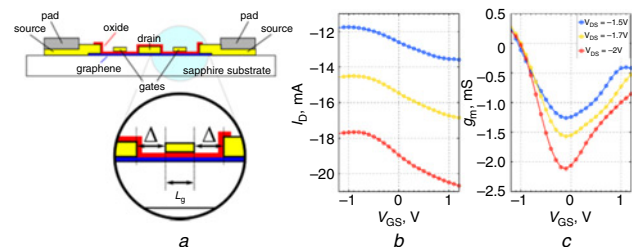


Fig. 1 Cross-section diagram of GFET and DC measurements

- a Cross-section diagram of GFET
- b I_D versus V_{GS} curve as a function of V_{DS} values for GFET with $\Delta = 125$ nm, $L_g = 250$ nm, 3 μm drain length and 20 μm channel width, respectively
- c g_m versus V_{GS} curves as function of V_{DS} values for the same GFET in (b)

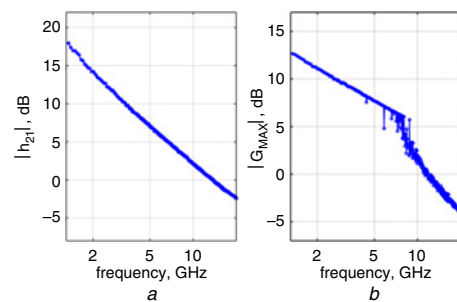


Fig. 2 Typical short-circuit current gain and maximum available gain of a GFET with $\Delta = 125$ nm and $L_g = 250$ nm

- a Intrinsic value of $|h_{21}|$ as a function of frequency
- b Intrinsic value of MAG as function of frequency

Keeping in mind that not only L_g but also Δ affects device performance, an in-depth investigation of such geometry dependence was carried out. A parametric analysis for each of the 24 fabricated GFET families has been performed by means of a statistical average on ten nominally identical devices. Table 1 summarises the denomination of each family and the corresponding Δ and L_g values. Figs. 3a and b show the 3D histograms of the cut-off frequency (f_T) and the maximum frequency of oscillation (f_{max}), respectively, obtained by averaging the data pertaining to the ten devices of the same family. All the reported values refer to the de-embedded measurements.

Table 1: Gate-drain/source distance (Δ) and gate length (L_g) of fabricated GFETs families and corresponding family denomination

L_g (nm)	Δ (nm)			
	125	250	500	750
125	AA	AB	AC	AD
250	BA	BB	BC	BD
500	CA	CB	CC	CD
1000	DA	DB	DC	DD
1500	EA	EB	EC	ED
2000	FA	FB	FC	FD

As shown in the maps in Fig. 3, the trends of f_T and f_{max} show similarities. In detail, when keeping constant L_g and decreasing Δ , an increase of both figures of merit is observed. Moreover, when keeping

constant Δ , both f_T and f_{max} do not increase monotonically with the scaling of the channel length. As regards the f_{max} trend, this result is in agreement with the literature [6, 9], while our work allows us to infer that both f_T and f_{max} are Δ and L_g dependent and that an optimum region exists where both figures of merit are maximised. The best values reached for f_T and f_{max} are 13.68 and 12.3 GHz, respectively. These values are obtained for devices belonging to the AB family ($\Delta = 250$ nm; $L_g = 125$ nm) and are not only more than ten times higher than those ones reached with the devices having the largest channel length (i.e. FD family: $\Delta = 750$ nm; $L_g = 2000$ nm) but also higher than the ones pertaining to smaller channel length devices. Contrarily to what could be expected from similarity with non-graphene-based FETs, devices with the shortest channel length do not show the best RF performance. The parasitic doping induced by the graphene/metal contacts negatively affects the electronic transport properties of the graphene nearby [7], causing an asymmetry of the transfer characteristics and, therefore, a worse GFET RF behaviour. Although the performance of the fabricated/compared devices is lower than that reported for state-of-the-art microwave GFETs, it shall be reasonably improved by adopting single-crystal CVD graphene [14] and optimised transfer [15] and does not affect the meaningfulness of the comparison. The comprehensive parametric/statistical investigation carried out in this Letter is thus instrumental for the future design of optimised graphene-based transistors.

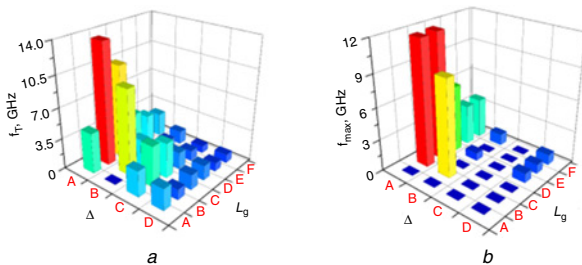


Fig. 3 Results of statistical and parametrical analysis: 3D map
 a Cut-off frequency (f_T) for the different GFET families
 b Maximum frequency of oscillation (f_{max}) for the different GFET families

Conclusion: In this Letter, 24 families of GFETs, fabricated on a single chip and differing for the gate-drain/source distance (Δ) and the gate length (L_g), have been characterised in both DC and RF/microwave regimes. A parametrical and statistical analysis has been performed, and the dependence of the main RF parameters on both Δ and L_g was evaluated. This Letter allowed us to demonstrate the existence of a region where the cut-off frequency and the maximum frequency of oscillation are optimised. Due to parasitic doping by metal contacts, devices with the shortest channel length exhibit the worst modulation of channel conductance, which is detrimental for the RF performance.

Acknowledgment: The authors thank Camilla Coletti for fruitful discussion of the results.

© The Institution of Engineering and Technology 2018
 Submitted: 27 April 2018 E-first: 29 June 2018
 doi: 10.1049/el.2018.5113

One or more of the Figures in this Letter are available in colour online.
 M.A. Giambra and V. Miseikis (CNIT-Consorzio Nazionale Interuniversitario per le Telecomunicazioni, via Moruzzi 1, 56124 Pisa, Italy)

✉ E-mail: marco.giambra@cnit.it

A. Benfante, L. Zeiss, R. Pernice, A.C. Cino, S. Stivala, E. Calandra and A.C. Busacca (Department of Energy, Information engineering and Mathematical models (DEIM), University of Palermo, Viale delle Scienze, Building 9, 90128 Palermo, Italy)

W.H.P. Pernice (Institute of Physics, University of Münster, Münster 48149, Germany)

M.H. Jang and J.-H. Ahn (School of Electrical and Electronic Engineering, Yonsei University, Seoul, Republic of Korea)

R. Danneau (Institute of Nanotechnology, Karlsruhe Institute of Technology, 76021 Karlsruhe, Germany)

References

- Schwierz, F.: 'Graphene transistors: status, prospects, and problems', *Proc. IEEE*, 2013, **101**, pp. 1567–1584
- Obradovic, B., Kotlyar, R., Heinz, F., *et al.*: 'Analysis of graphene nanoribbons as a channel material for field-effect transistors', *Appl. Phys. Lett.*, 2006, **88**, (14)
- Luisier, M., and Klimeck, G.: 'Performance analysis of statistical samples of graphene nanoribbon tunneling transistors with line edge roughness', *Appl. Phys. Lett.*, 2009, **94**, (22)
- Gan, A., Performance, H., Russo, S., *et al.*: 'Influence of the source-gate distance on the AlGaIn/GaN HEMT performance', *Trans. Electron Devices*, 2007, **54**, (5), pp. 1071–1075
- Deng, X., Zhang, B., Li, Z., *et al.*: 'Two-dimensional analysis of the surface state effects in 4H-SiC MESFETs', *Microelectron. Eng.*, 2008, **85**, (2), pp. 295–299
- Wu, Y., Jenkins, K.A., Valdes-Garcia, A., *et al.*: 'State-of-the-art graphene high-frequency electronics', *Nano Lett.*, 2012, **12**, (6), pp. 3062–3067
- RyoNouchi, K.T., and Saito, T.: 'Determination of carrier type doped from metal contacts to graphene by channel-length-dependent shift of charge neutrality points', *Appl. Phys. Express*, 2011, **4**, p. 35101
- Huard, B., Stander, N., Sulpizio, J.A., *et al.*: 'Evidence of the role of contacts on the observed electron-hole asymmetry in graphene', *Phys. Rev. B*, 2008, **78**, (12), p. 121402
- Lin, Y.-M., Jenkins, K.A., Valdes-Garcia, A., *et al.*: 'Operation of graphene transistors at gigahertz frequencies', *Nano Lett.*, 2009, **9**, (1), pp. 422–426
- Pallecchi, E., Benz, C., Betz, A.C., *et al.*: 'Graphene microwave transistors on sapphire substrates', *Appl. Phys. Lett.*, 2011, **99**, (11), p. 113502
- Wang, H., Hsu, A., Lee, D.S., *et al.*: 'Delay analysis of graphene field-effect transistors', *Electron Device Lett.*, 2012, **33**, (3), pp. 324–326
- Kim, K.S., Zhao, Y., Jang, H., *et al.*: 'Large-scale pattern growth of graphene films for stretchable transparent electrodes', *Nature*, 2008, **457**, (7230), pp. 706–710
- Hsu, A., Wang, H., Kim, K.K., *et al.*: 'Impact of graphene interface quality on contact resistance and RF device performance', *Electron Device Lett.*, 2011, **32**, (8), pp. 1008–1010
- Miseikis, V., Bianco, F., David, J., *et al.*: 'Deterministic patterned growth of high-mobility large-crystal graphene: a path towards wafer scale integration', *2D Mater.*, 2017, **4**, (2), p. 21004
- Banszerus, L., Schmitz, M., Engels, S., *et al.*: 'Ultra-high-mobility graphene devices from chemical vapor deposition on reusable copper', *Sci. Adv.*, 2015, **1**, (6), pp. 1–6
- Wang, L., Meric, L., Huang, P.Y., *et al.*: 'One-dimensional electrical contact to a two-dimensional material', *Science*, 2013, **342**, (6158), pp. 614–617